THE JOURNAL OF BIOLOGICAL CHEMISTRY
Vol. 280, No. 36, Issue of September 9, pp. 31913–31923, 2005
Printed in U.S.A.

Phosphorylation of Coronin 1B by Protein Kinase C Regulates Interaction with Arp2/3 and Cell Motility*

Received for publication, April 15, 2005, and in revised form, June 7, 2005
Published, JBC Papers in Press, July 18, 2005, DOI 10.1074/jbc.M504146200

Liang Cai, Nicholas Holoweckyj, Michael D. Schaller, and James E. Bear‡

From the Lineberger Comprehensive Cancer Center and Department of Cell & Developmental Biology, University of North Carolina Chapel Hill School of Medicine, Chapel Hill, North Carolina 27599

Coronins are a conserved family of WD repeat-containing, actin-binding proteins that regulate cell motility in a variety of model organisms. Our results show that Coronin 1B is a ubiquitously expressed member of the mammalian Coronin gene family that co-localizes with the Arp2/3 complex at the leading edge of fibroblasts, and co-immunoprecipitates with this complex. Pharmacological experiments show that the interaction between Coronin 1B and the Arp2/3 complex is regulated by protein kinase C (PKC) phosphorylation. Coronin 1B is phosphorylated by PKC both *in vitro* and *in vivo*. Using tryptic peptide mapping and mutagenesis, we have identified serine 2 (Ser-2) on Coronin 1B as the major residue phosphorylated by PKC *in vivo*. Rat2 fibroblasts expressing the Coronin 1B S2A mutant show enhanced ruffling in response to phorbol 12-myristate 13-acetate (PMA) and increased speed in single cell tracking assays. Cells expressing the Coronin 1B S2D mutant have attenuated PMA-induced ruffling and slower cell speed. Expression of the S2A mutant partially protects cells from the inhibitory effects of PMA on cell speed, whereas expression of the S2D mutant renders cells hypersensitive to its effects. These data demonstrate that Coronin 1B regulates leading edge dynamics and cell motility in fibroblasts, and that its ability to control motility and interactions with the Arp2/3 complex are regulated by PKC phosphorylation at Ser-2. Furthermore, Coronin 1B phosphorylation is responsible for a significant fraction of the effects of PMA on fibroblast motility.

The dynamic re-organization of the actin cytoskeleton is required for many processes including migration, endocytosis, and intracellular junction formation. Coronins are a conserved family of WD repeat-containing, actin-binding proteins that regulate migration and other actin-dependent processes in model organisms. Mammalian genomes contain at least six Coronin genes, however, little is known about the molecular function or regulation of Coronins in mammalian cell motility.

The founding member of the Coronin protein family was discovered in *Dictyostelium* as an F-actin-binding protein present in a contracted myosin-actin preparation (1). Subsequent gene knock-out studies showed that this protein was involved in cell motility and cytokinesis (2). *Dictyostelium* cells deficient in Coronin move at about half the rate of the wild-type controls and have a high frequency of failed cytokinesis. The protein is localized at the leading edge of motile cells. In addition to motility defects, Coronin null cells also have strong defects in fluid phase endocytosis (3).

Yeast also has a Coronin protein that binds to F-actin *in vitro* and localizes *in vivo* to dynamic actin structures such as actin patches (4, 5). Unlike *Dictyostelium*, disruption of the single Coronin gene (*CRN1*) in yeast does not lead to gross defects in growth or cytoskeletal organization. However, when a *crn1* mutation is combined with a mutation in the gene encoding Cofilin (*cof1–22*), a protein involved in actin filament turnover, synthetic defects in growth and cytoskeletal organization are observed (5). Overexpression of Coronin in yeast induces the formation of aberrant actin loops and causes lethality (6). Purified yeast Coronin binds directly to the Arp2/3 complex via its coiled-coil domain and inhibits Arp2/3-mediated actin nucleation *in vitro*. In support of these *in vitro* studies, mutations in the *CRN1* gene genetically synergize with mutations in the subunits of the Arp2/3 complex.

Coronin has also been studied in other model organisms. In *Drosophila*, mutations in Coronin cause disruptions in the actin cytoskeleton of the embryonic imaginal disks and an early pupal lethal phenotype, indicating that this gene is essential for morphogenesis in this organism (7). In *Xenopus*, Coronin localizes to the periphery of fibroblastic cells and, like *Dictyostelium* and yeast Coronins, co-sediments with F-actin *in vitro* (8). Also, the coiled-coil region at the C terminus of *Xenopus* Coronin has been shown to mediate oligomerization (9). Expression of a putative dominant negative construct containing the five canonical WD repeats from *Xenopus* Coronin leads to defects in cell spreading and Rac-induced lamellipodial formation (8).

Several mammalian members of the Coronin family have been described (10). For clarity, we have adopted the Human Genome Organization (HUGO) nomenclature for mammalian Coronin genes (www.gene.ucl.ac.uk/nomenclature/genefamily/coronin.html). Coronin 1A (also known as p57 or Coronin-1) was the first Coronin to be identified in mammals and is highly expressed in cells of the hematopoietic lineage as well as parts of the nervous system (11). This protein is a substrate for PKC both *in vitro* and *in vivo*; however, the sites that are phosphorylated are unknown and the functional significance of phosphorylation has not been well characterized (12). Coronin 1B (also known as $\text{Coronin}_{\text{SE}}$ or Coronin-2) was discovered as a carbachol-stimulated phosphoprotein in rabbit parietal cells (13). Carbachol acts via a protein kinase C (PKC)[1] pathway in

* This work was supported by funds from the V Foundation Scholar award (to J. E. B.) and National Institutes of Health Grants CA90901 and HL45100 (to M. D. S.). The costs of publication of this article were defrayed in part by the payment of page charges. This article must therefore be hereby marked "*advertisement*" in accordance with 18 U.S.C. Section 1734 solely to indicate this fact.

‡ To whom correspondence should be addressed: Lineberger Cancer Center, University of North Carolina Chapel Hill School of Medicine, CB 7295, Chapel Hill, NC 27599-7295. Tel.: 919-966-5471; Fax: 919-966-3015; E-mail: jbear@email.unc.edu.

[1] The abbreviations used are: PKC, protein kinase C; IP, immunoprecipitation; co-IP, co-immunoprecipitation; PMA, phorbol 12-myristate 13-acetate; GFP, green fluorescent protein; GST, glutathione *S*-transferase; MOPS, 3-(*N*-morpholino)propanesulfonic acid.

this cell type to regulate secretion. Recently, this gene was identified in a microarray-based screen for genes up-regulated in a neural regeneration model (14). Overexpression of Coronin 1B induced neurite extension in several neuronal cell lines, whereas reduced expression via RNA interference caused a reduction in outgrowth. Two-dimensional gel electrophoresis studies suggest that Coronin 1C (Coronin-3) is also phosphorylated *in vivo* (15).

The potential PKC regulation of mammalian Coronins is intriguing because this family of Ser/Thr kinases regulates migration in many cell types. Activation of classic and novel isoforms of PKC by the phorbol ester phorbol 12-myristate 13-acetate (PMA) in some cell types increases cell migration, whereas in other cell types, it is inhibitory (16). These opposing effects are likely because of the complement of PKC isoforms and/or substrate proteins expressed in a given cell type (17). PMA is thought to exert its effects on migration by changing adhesiveness and/or actin architecture at the leading edge (18, 19). PMA also regulates other actin-based motility events such as neurite outgrowth and endosome rocketing (20, 21). Despite the clear importance of PKC in cell motility, a relatively small number of PKC substrate proteins have been thoroughly characterized in terms of the residues phosphorylated and functional significance of their phosphorylation in the control of motility. In this work, we have identified serine 2 as the major *in vivo* PKC phosphorylation site on Coronin 1B, and demonstrate that phosphorylation regulates the interaction between Coronin 1B and the Arp2/3 complex. Furthermore, we show that Ser-2 phosphorylation of Coronin 1B regulates PMA-induced ruffling and cell migration.

EXPERIMENTAL PROCEDURES

Materials—Commercial antibodies were obtained from Cell Signaling Technologies ($pSer^{PKC}$), Upstate Biotechnology (p34-Arc), Roche (GFP), and Sigma (9E10/Myc). Alexa Fluor 568 phalloidin was from Molecular Probes. Cell lines were from ATCC. PKC inhibitors Ro32-0432 and Gö6976 were from Calbiochem. Protease and phosphatase inhibitors (phenylmethylsulfonyl fluoride, 1,10-phenanthroline, aprotinin, leupeptin, sodium fluoride, and sodium orthovanadate) were from Sigma. All other materials were from Fisher Scientific unless otherwise indicated.

TaqMan Quantitative Real-time PCR—Total RNA was isolated from murine tissues using a Qiagen RNeasy Isolation kit according to the manufacturer's protocol. Reverse transcription into cDNA was done in a 20-μl volume using oligo$(dT)_{12–18}$ Primer, 10 mM dNTP mixture, and Improm-II Reverse Transcriptase (Promega) according to the manufacturer's instructions. PCR were carried out in a 20-μl volume consisting of 10 μl of Universal Master Mix No AmpErase UNG (Applied Biosystems), 0.25 μg of fluorogenic probe (Mm00486998_m1[1A], Mm00488552_g1[1B], Mm00488558_m1[1C], Mm00619135_m1[2A], Mm00558512_m1[2B], Mm00504152_m1[POD], Applied Biosystems), and 8 μl of diluted cDNA (~80 ng of total RNA/reaction). The PCRs were carried out under standard conditions in a 20-μl volume in duplicate for each sample in the ABI Prism 7700 Sequence Detection System (Applied Biosystems). The number of PCR cycles needed to reach the fluorescence threshold was determined in duplicate for each cDNA, averaged, and then normalized against a reference gene, 18 S (4333760–0311007 Applied Biosystems), to yield the cycle number at which fluorescence was reached (C_t). For the absolute copy number of Coronin 1A, 1B, 1C, 2A, 2B, and POD, 4-fold dilutions of the respective mouse full-length cDNAs were used to generate a standard curve (22). All tissue samples tested were within the linear range (19–38 cycles) of the assay.

Molecular Cloning—PCR and subcloning were performed using standard methods. Detailed methods and primer sequences are available upon request. WT1B-EGFP was constructed by amplifying the coding sequence of human Coronin 1B and cloning it into a pMSCV-based retroviral vector (23). S2A-EGFP and S2D-EGFP were generated from WT1B-EGFP by site-directed mutagenesis using mutation-encoding primers. Coronin 1B-Myc was generated by subcloning the Coronin 1B coding sequence into a pMSCV vector containing a C-terminal Myc tag.

Cell Culture, Transient Transfection, and Retroviral Transduction—HEK293 and Swiss 3T3 cells were cultured in Dulbecco's modified Eagle's medium-H supplemented with 10% fetal bovine serum (HyClone), 100 units/ml penicillin, 100 μg/ml streptomycin, and 292 μg/ml glutamine. Rat2 and NIH3T3 cells were cultured in the same media supplemented with 5% fetal bovine serum or 10% calf serum (HyClone), respectively. HEK293 cells were transiently transfected with plasmids using FuGENE 6 transfection reagent (Roche) according to the manufacturer's protocol. Retroviral packaging, infections, and fluorescence-activated cell sorting were performed as described previously (23).

Immunoprecipitation—Cells were washed twice with phosphate-buffered saline and lysed with a KCl buffer (20 mM HEPES, pH 7.0, 100 mM KCl, 0.5% Nonidet P-40, 1 mM EDTA, 1 mM phenylmethylsulfonyl fluoride, 10 μg/ml 1,10-phenanthroline, 10 μg/ml aprotinin, 10 μg/ml leupeptin, 10 mM sodium fluoride, and 2 mM sodium orthovanadate). Lysates were cleared at 13,000 $\times$ *g* for 5 min and incubated with 0.5 μg of primary antibody for 1 h at 4 °C, followed by the addition of 20 μl of 50% slurry of ImmunoPure-immobilized protein A/G beads (Pierce) and further incubation at 4 °C for an additional hour. Beads were pre-blocked with 1 mg/ml bovine serum albumin and washed extensively with the KCl buffer prior of usage. The immune complexes were collected, washed with the KCl buffer three times, separated by SDS-PAGE, and transferred to a polyvinylidene difluoride membrane (Bio-Rad) for Western blotting.

Recombinant Protein Production—His_6-tagged Coronin 1B (His1B) was generated by PCR cloning the coding sequence of human Coronin 1B into pQE-80L (Qiagen). GST-tagged full-length (GST1B) or the C-terminal fragment of Coronin 1B were cloned by PCR into pGEX-6P1 (Amersham Biosciences). For protein production, cells were grown to mid-log and expression was induced with 0.5 mM isopropyl 1-thio-β-D-galactopyranoside for 6 h at room temperature. Bacteria was harvested and sonicated in lysis buffer (50 mM HEPES, pH 7.4, 0.5% Triton X-100, 0.5 M NaCl, 5 mM 2-mercaptoethanol, 1 mM phenylmethylsulfonyl fluoride, 10 μg/ml 1,10-phenanthroline, 10 μg/ml aprotinin, 10 μg/ml leupeptin, and 10 mM imidazole). His1B was purified by affinity chromatography using nickel-chelated agarose (Pierce). Lysate, cleared at 20,000 $\times$ *g* for 20 min, was applied to a nickel-chelated agarose column, and washed using the lysis buffer containing 40 mM imidazole. His1B was eluted with 500 mM imidazole in 50 mM HEPES, pH 7.4, 0.5 M NaCl. GST-tagged proteins were purified by affinity chromatography using immobilized glutathione beads (Pierce) according to the manufacturer's protocol, and the GST tag was on-column removed by PreScission protease (Amersham Biosciences). The C-terminal region of mouse Coronin 1B (394–484 amino acids) was PCR cloned into pMAL-c2g vector (New England Biolabs). Maltose-binding protein was purified by affinity chromatography using amylose resin (New England Biolabs) according to the manufacturer's protocol.

In Vitro Phosphorylation—2 μg of recombinant protein was incubated with ~0.5 μg of PKCα (Panvera or Sigma) in 100 μl of kinase assay buffer (7.2 mM HEPES, pH 7.4, 3.6 mM $MgCl_2$, 0.18 mM EGTA, 0.1% Triton X-100, 0.63 mM $CaCl_2$, 0.1 μM ATP, 0.5 μM PMA, 120 μM phosphatidylserine) containing 10 μCi of [γ-^{32}P]ATP for 30 min at 30 °C (24). Reactions were terminated by adding an equal volume of 2$\times$ sample buffer. The samples were subjected to SDS-PAGE and transferred to a nitrocellulose membrane for autoradiography and peptide mapping.

In Vivo Phosphorylation—Cells were serum starved for 12 h before metabolic labeling, and then incubated with [^{32}P]orthophosphoric acid (Amersham Biosciences) in phosphate-free minimum essential medium (Sigma). After 8 h, cells were treated with or without 100 nM PMA for 30 min and lysed with RIPA buffer (50 mM Tris-HCl, pH 7.3, 150 mM NaCl, 1% IPEGAL, 0.5% deoxycholate, 1 mM EDTA, 1 mM phenylmethylsulfonyl fluoride, 10 μg/ml 1,10-phenanthroline, 10 μg/ml aprotinin, 10 μg/ml leupeptin, 1 mM α-naphthyl acid phosphate, 10 mM sodium fluoride, and 2 mM sodium orthovanadate). The 13,000 $\times$ *g* cleared lysates were immunoprecipitated as described above. The immune complexes were separated by SDS-PAGE and transferred to a nitrocellulose membrane for autoradiography and peptide mapping.

Peptide Mapping—Peptide mapping was performed as described previously (25, 26). Briefly, appropriate protein bands were cut from the nitrocellulose membrane and digested with L-1-tosylamido-2-phenylethyl chloromethyl ketone-treated trypsin (95%, 284 units/mg; Worthington) in 0.05 M NH_4HCO_3, pH 7.8, at 37 °C for 24 h. The peptides were washed and dried using a speed vacuum centrifuge, and spotted onto cellulose thin layer chromatography plate (Merck KGaA, Germany) for two-dimensional mapping using pH 8.9 buffer (ammonium carbonate, 10 g/liter) for electrophoresis in the first dimension and phosphochromatography buffer (*n*-butanol:pyridine:glacial acetic acid:deionized water, 75:50:15:60) for chromatography in the second dimension. After

that the thin layer chromatography plates were dried completely for autoradiography.

Coro1B Antibody Production and Affinity Purification—Rabbits were immunized with a GST fusion protein containing the human Coronin 1B C-terminal region (394–489 amino acids) by Covance. Serum was affinity purified against maltose-binding fusion protein containing the equivalent region of mouse Coronin 1B to ensure cross-reactivity. This myelin basic fusion protein was purified in a buffer containing 10 mM MOPS, pH 7.5, and 60 mM sodium citrate, which was used for direct coupling to UltraLink biosupport media (Pierce) according to the manufacturer's protocol. The column was washed extensively with 10 mM Tris, pH 7.5, 100 mM glycine, pH 2.5, and 100 mM triethylamine, pH 11.5, with neutralizing washes between. Crude serum was diluted 10-fold in 10 mM Tris, pH 7.5, and passed through the column three times. The column was washed with 10 mM Tris, pH 7.5, and then with 500 mM NaCl, 10 mM Tris, pH 7.5. Antibodies were eluted sequentially with 100 mM glycine, pH 2.5, followed by 100 mM triethylamine, pH 11.5. The antibody-containing fractions were neutralized, combined, and dialyzed against phosphate-buffered saline.

Immunofluorescence Microscopy—For immunofluorescent staining, the cells were fixed, stained, and mounted as described previously (23). Cells were stained in various combinations with Alexa Fluor 568 phalloidin for F-actin (1:400 dilution), p34-Arc (1:400 dilution), or affinity purified Coro1B antibody (1:200 dilution). Images were captured using a Nipkow-type spinning disk confocal scan head (Yokogawa CSU-10) attached to an inverted microscope (model IX-81, Olympus) equipped with a ×60 1.45 NA objective, a CCD camera (model C4742–80-12AG, Hamamatsu), and controlled by AQM Advance 6 software (Kinetic Imaging, Ltd.). The extended depth of focus plugin (bigwww.epfl.ch/demo/edf/) for ImageJ was used to combine multiple images from a *z*-stack (8 slices, 150 nm interval) into a single in-focus image. Images were combined and annotated in Photoshop for presentation.

PMA-induced Ruffling Assay—To quantify ruffling, Rat2 cells were serum-starved overnight, stimulated with 100 nM PMA, fixed at various times as indicated, and stained with Alexa Fluor 568 phalloidin to visualize membrane ruffles. At least 200 cells were counted for each time point.

Single Cell Tracking—Tracking was performed as described previously (23). To increase data throughput, 10 different fields (containing ~10–20 cells per field) were simultaneously recorded using an automated X-Y stage (Prior). To avoid bias in the analysis, every cell in each movie that met the tracking criteria (did not divide, was completely within the field of view for the entire experiment, and did not touch another cell for more than two frames) was tracked using Tracking Analysis software (Kinetic Imaging, Ltd.) with the point-click mode. Cell speed was calculated using the Tracking Analysis software and directional persistence was calculated using custom Matlab macros (a kind gift of B. Harms, MIT). Data were analyzed using PRISM (GraphPad, Inc.) for statistical analysis.

RESULTS

As a first step in understanding the role of mammalian Coronins in cell motility, we used quantitative real-time PCR to compare expression patterns of the genes across mouse tissues. An advantage of this technique is the ability to quantitatively compare expression between genes, as well as across tissues. Our data indicate that the most widely expressed mammalian Coronin gene is *CORONIN 1B*, which is expressed at high levels across most tissues (Fig. 1*B*). A full characterization of mammalian Coronin gene expression using this technique will be presented elsewhere.[2] To study Coronin 1B at the protein level, a polyclonal antibody was raised against the unique region and the coiled-coil region of human Coronin 1B (Fig. 1*A*). HEK293 cells were transient transfected with all six Coronin genes tagged with GFP at the C terminus. The different Coronins were enriched by immunoprecipitation (IP) using a GFP antibody and blotted with the affinity purified Coro1B antibody. This antibody specifically recognizes Coronin 1B and does not cross-react with the other related Coronins (Fig. 1*C*). Interestingly, the endogenous Coronin 1B was co-immunoprecipitated (co-IP) with Coronin 1B-GFP. The endogenous protein was co-immunoprecipitated only from cells transfected with Coronin 1B-GFP and not with any of the other Coronin constructs, suggesting only homo-oligomerization had occurred. To confirm this result, we co-transfected cells with the complete set of Coronin genes tagged with GFP and Coronin 1B-Myc. Immunoprecipitation with a Myc antibody co-precipitated only Coronin 1B-GFP and none of the other Coronins (Fig. 1*D*). Together, these experiments strongly suggest that Coronin 1B exclusively homo-oligomerizes and does not form complexes with the other Coronins. Whereas other Coronins have been shown to homo-oligomerize via their coiled-coil motif *in vivo* (27), these data are the first to address the specificity of oligomerization between members of this protein family.

To examine the localization of Coronin 1B, we used our affinity purified antibody for immunofluorescent staining and compared the localization of the endogenous protein to the GFP-tagged form in Rat2 fibroblasts (Fig. 1*E*). Coronin 1B is localized to the leading edge in fibroblasts, as well as weakly along actin stress fibers. The localization of the GFP-tagged form is indistinguishable from the endogenous protein. This observation, along with the co-IP experiment described above, suggests that Coronin 1B can tolerate tagging with GFP at the C terminus.

In yeast, Coronin and the Arp2/3 complex biochemically and genetically interact, but this interaction has not been demonstrated in mammalian systems (6). To examine this interaction, we first performed immunofluorescent co-localization between Coronin 1B and p34-Arc (a component of the Arp2/3 complex). These two proteins strongly and completely co-localize at the leading edge of fibroblasts (Fig. 2*A*). To test for a biochemical interaction between Coronin 1B and the Arp2/3 complex, we performed a reciprocal co-IP between Coronin 1B and the p34-Arc subunit of the Arp2/3 complex. We saw a robust, reciprocal co-IP between the endogenous Coronin 1B and p34-Arc in Rat2 fibroblasts (Fig. 2*B*). This result was also obtained in HEK293, Swiss 3T3, and NIH3T3 cells, suggesting that this interaction is generally observed in many cell types (data not shown). Control rabbit antibodies did not IP either protein (Fig. 2, *B* and *C*). We also detected co-IP between Coronin 1B and the Arp2 and p41Arc subunits of the Arp2/3 complex (data not shown), suggesting that our results are not specific for p34-Arc, but reflect an interaction between Coronin 1B and the Arp2/3 complex. As an additional control, we were also able to show co-IP between GFP-tagged Coronin 1B and p34-Arc using GFP antibodies (Fig. 6*B*). We could not detect actin in the immunocomplex by blotting, but to exclude the possibility that this interaction is simply bridged through F-actin, we pretreated cells with Latrunculin B to disrupt F-actin prior to making the lysate for IP and saw no change in the interaction (data not shown).

Because Coronins have been shown to be PKC substrates *in vitro* and *in vivo* (12, 13), we tested whether phosphorylation modulates the interaction between Coronin 1B and the Arp2/3 complex. With 100 nM PMA treatment, this interaction is strongly decreased relative to untreated Rat2 cells (Fig. 2*C*). To establish that the PMA stimulation was acting through a kinase pathway, we used an anti-phosphoserine antibody raised against a phosphopeptide corresponding to the PKC consensus site. This antibody ($pSer^{PKC}$) recognizes phosphorylated Coronin 1B immunoprecipitated by our affinity purified Coro1B antibody (Fig. 2*C*). Mutant analysis as described below confirmed the specificity of this antibody for phospho-Coronin 1B. Further evidence for the specific involvement of PKC in regulating Coronin 1B-Arp2/3 interactions comes from treatment with two well established PKC inhibitors (28, 29). Pretreatment of cells with a pan-PKC inhibitor (Ro32–0432) blocked

[2] L. Cai, N. Holoweckyj, and J. E. Bear, unpublished observations.

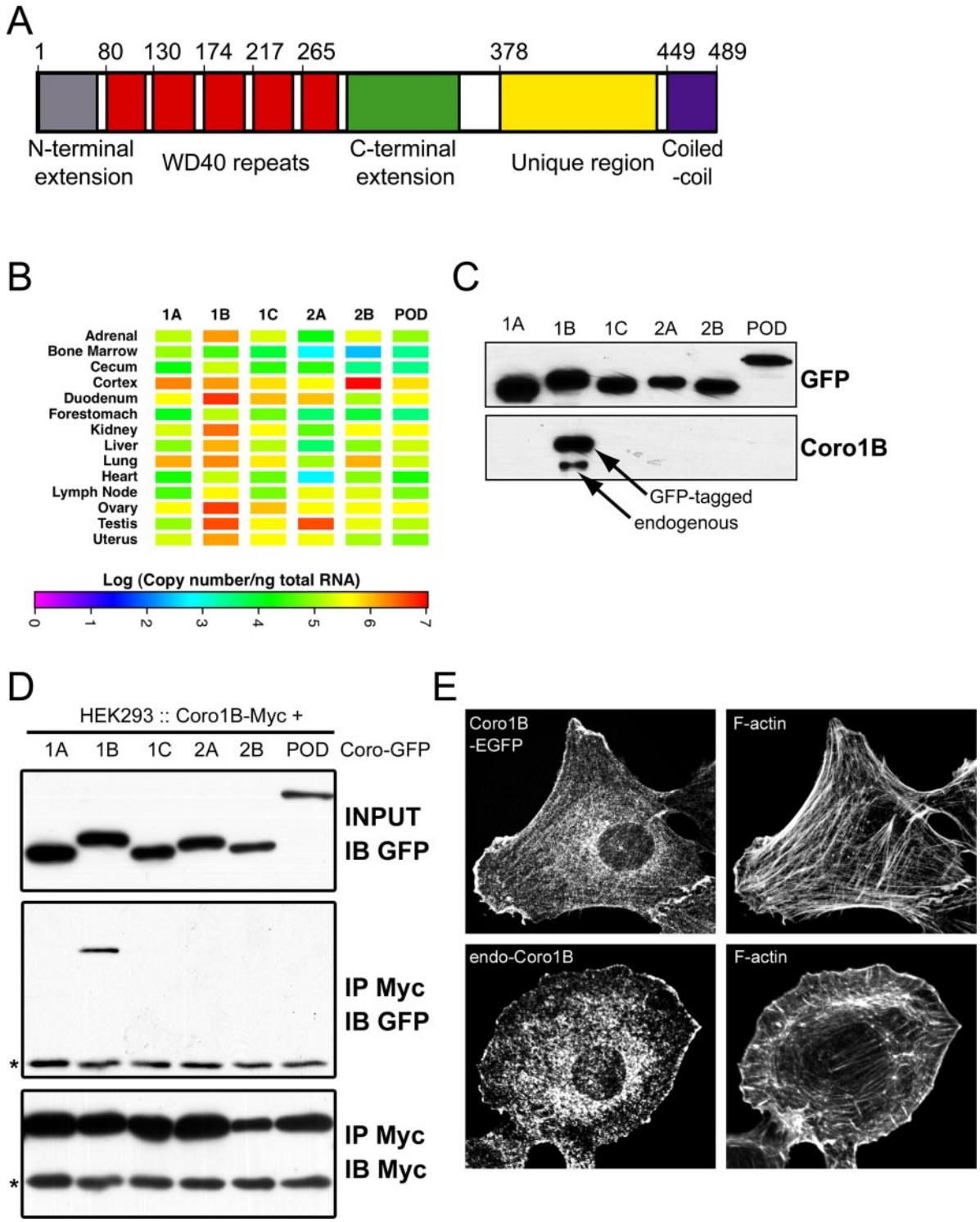

FIG. 1. **Expression, oligomerization, and localization of Coronin 1B.** *A*, schematic diagram of Coronin 1B. *B*, quantitative heat map of Coronin gene expression across mouse tissues using quantitative real-time PCR. Color scale indicates $\log_{10}$ value of the copy number of mRNA per ng of total RNA for each Coronin gene based on cDNA standard curves derived as described under "Experimental Procedures." *C*, homo-oligomerization of Coronin 1B. HEK293 were transfected with the complete set of GFP-tagged Coronins, immunoprecipitated using a GFP antibody, and blotted with GFP antibody or affinity purified Coronin 1B antibody. *D*, exclusive homo-oligomerization of Coronin 1B-GFP and Coronin 1B-Myc. HEK293 cells were co-transfected with the complete set of GFP-tagged Coronin genes and Coronin 1B-Myc, immunoprecipitated using a Myc antibody, and blotted for GFP or Myc. *Asterisks* indicate IgG heavy chain as a loading control. *E*, localization of GFP-tagged and endogenous Coronin 1B in Rat2 fibroblasts. *IB*, immunoblotted.

PMA-stimulated phosphorylation of Coronin 1B and restored the co-IP with p34-Arc. Interestingly, Gö6976 (which inhibits the α and βI isoforms of PKC) did not block phosphorylation or restore co-IP of p34-Arc, suggesting that a novel isoform of PKC (δ, ϵ, or θ) may be responsible for the PMA-induced phosphorylation of Coronin 1B *in vivo*. Together, these experiments suggest that the interaction between Coronin 1B and the Arp2/3 complex is regulated through PKC phosphorylation of Coronin 1B.

Because the phosphorylation status of Coronin 1B is critical for interaction with the Arp2/3 complex, we sought to identify the residues that are phosphorylated *in vivo*. As a first step, we did an *in vitro* kinase assay using purified PKC and His-tagged

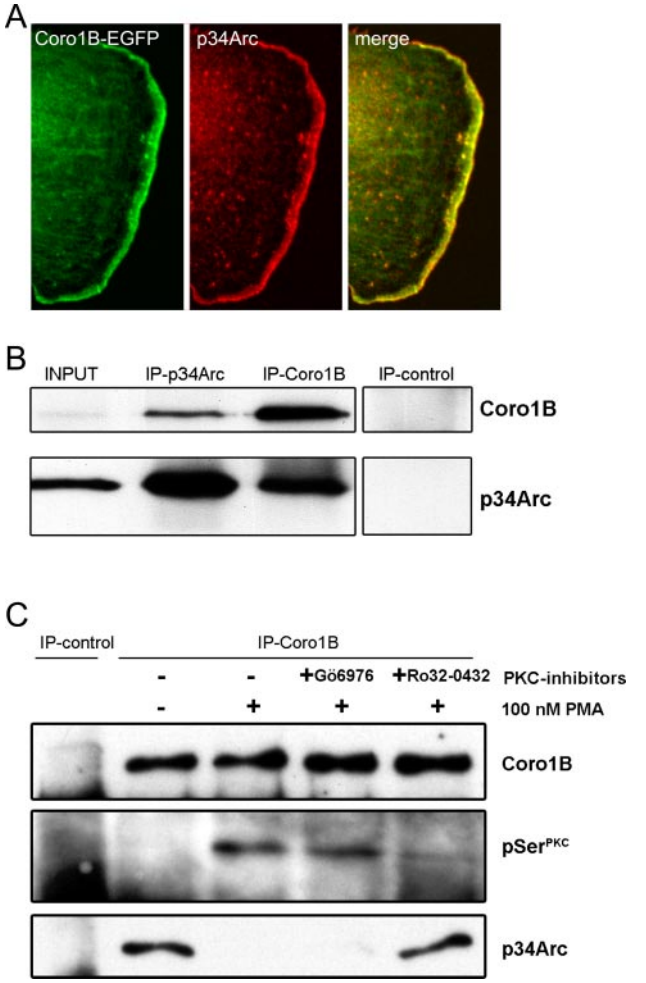

FIG. 2. **Coronin 1B interacts *in vivo* with the Arp2/3 complex in a PKC phosphorylation-dependent manner.** *A*, Coronin 1B co-localization with the p34-Arc subunit of the Arp2/3 complex at the leading edge of Rat2 fibroblasts. *B*, reciprocal co-immunoprecipitation between endogenous Coronin 1B and p34-Arc in Rat2 cell lysates. Rabbit IgG was used as a control for immunoprecipitation in *panels B* and *C*. *C*, pharmacological modulation of interaction between Coronin 1B and p34-Arc. Upon PMA stimulation (100 nM), Coronin 1B is phosphorylated (*pSer^{PKC} blot*) and the co-IP between Coronin 1B and the Arp2/3 complex strongly decreases (*p34-Arc blot*). Both effects are blocked by the pan-PKC inhibitor, Ro32-0432 (1 μM), but not by Gö6976 (30 μM), which inhibits only PKCα and β1.

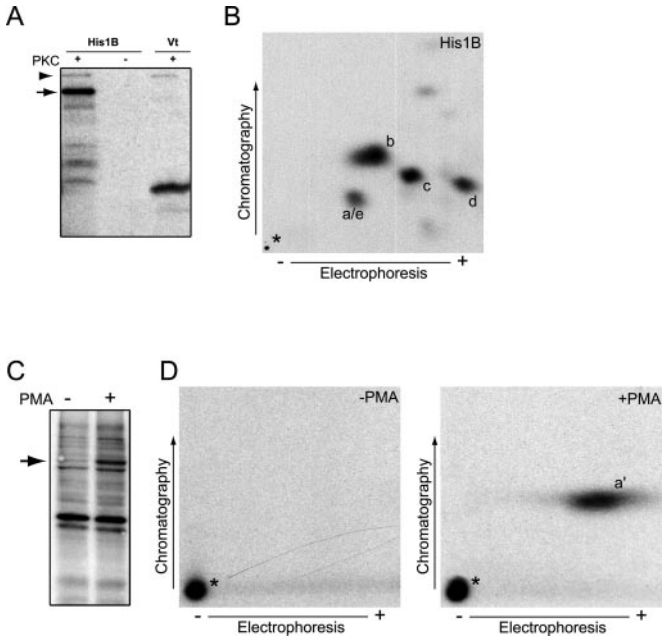

FIG. 3. **Coronin 1B is robustly phosphorylated both *in vitro* and *in vivo*.** *A*, recombinant His-Coronin 1B is phosphorylated by PKCα *in vitro* (*arrow*). The phosphorylation of chicken vinculin tail (*Vt*; amino acids 881–1135) served as a positive control. PKCα autophosphorylation is indicated by the *arrowhead*. *B*, *in vitro* phosphorylated His-Coronin 1B subjected to tryptic peptide mapping. The *asterisk* indicates origin. Spots *a–e* showed a consistent pattern across multiple experiments. *C*, GFP-tagged Coronin 1B was immunoprecipitated from ^{32}P metabolically labeled HEK293 cells treated with and without 100 nM PMA (*arrow* indicates Coro1B-EGFP). *D*, tryptic peptide map of a sample from *C*.

Coronin 1B. Recombinant Coronin 1B is strongly phosphorylated in this reaction (Fig. 3*A*). Similar results were obtained using GST-tagged Coronin 1B (see below). As a positive control, we used a fragment of vinculin that has been reported to be an *in vitro* PKC substrate (24). Tryptic peptide mapping shows that 4 to 5 sites on Coronin 1B are phosphorylated *in vitro* (Fig. 3*B*). To examine *in vivo* Coronin 1B phosphorylation, we immunoprecipitated GFP-tagged Coronin 1B from metabolically labeled HEK293 cells. Upon PMA stimulation, Coronin 1B was strongly phosphorylated (Fig. 3*C*). Tryptic peptide mapping indicated that there is a single major site phosphorylated *in vivo* (Fig. 3*D*).

Comparison of the *in vitro* and *in vivo* tryptic peptide maps indicated that the *in vivo* site did not appear to match any of the *in vitro* sites. We considered two possible explanations for this observation: first, that PKC does not phosphorylate the site *in vitro* that is utilized *in vivo*, or second, that the spot had shifted because of an extra sequence on the peptide from the His_6 or GST tag. Comparison of the tryptic peptide maps of *in vivo* phosphorylated Coronin 1B and *in vitro* phosphorylated His1B or (GST)1B provide strong evidence for the latter possibility. We used pairwise mixing of samples to compare the maps of *in vitro* and *in vivo* phosphorylated proteins (Fig. 4, *A–D*). Both the *in vitro* samples showed spots b, c, d, and e (Fig. 4*C*) that were absent in the *in vivo* labeled sample. Furthermore, we discovered that each sample contained a unique spot (a, a′, and a″). It is important to note that, in the case of (GST)1B, the N-terminal GST tag was removed by cleavage prior to the phosphorylation reaction leaving five residual amino acids. Because each sample has a unique N-terminal tryptic peptide because of fusion of the His or GST tags (Fig. 4*E*), we postulated that a serine or threonine residue common to all of these peptides, Ser-2 in the native protein, might be the *in vivo* phosphorylated residue. Further evidence for this hypothesis came from the predicted migration properties of the N-terminal peptides. A theoretical peptide map of these peptides, constructed based on established formulas for the relative migration of tryptic peptides, agreed with our experimental observations (Fig. 4*F*) (25).

To test the hypothesis that Ser-2 is the major *in vivo* phosphorylation site of Coronin 1B, this residue was mutated to alanine in our GFP-tagged Coronin 1B construct and transfected into HEK293 cells. This mutant, S2A, was immunoprecipitated from metabolically labeled cells stimulated with PMA and subjected to peptide mapping (Fig. 5*A*). The prominent phosphopeptide spot, a′, was absent in the S2A sample, suggesting that this is the major phosphorylation site *in vivo*. To exclude the possibility that the Ser-2 mutation changes the conformation of Coronin 1B and masks the actual phosphorylation site, we did an *in vitro* kinase assay on immunoprecipitated wild type or S2A Coronin 1B-GFP from unlabeled HEK293 cells (Fig. 5*B*). No phosphorylation was observed in the absence of purified PKC, indicating that no endogenous PKC was co-immunoprecipitated under these conditions. The wild-type Coronin 1B-GFP showed a prominent band at the

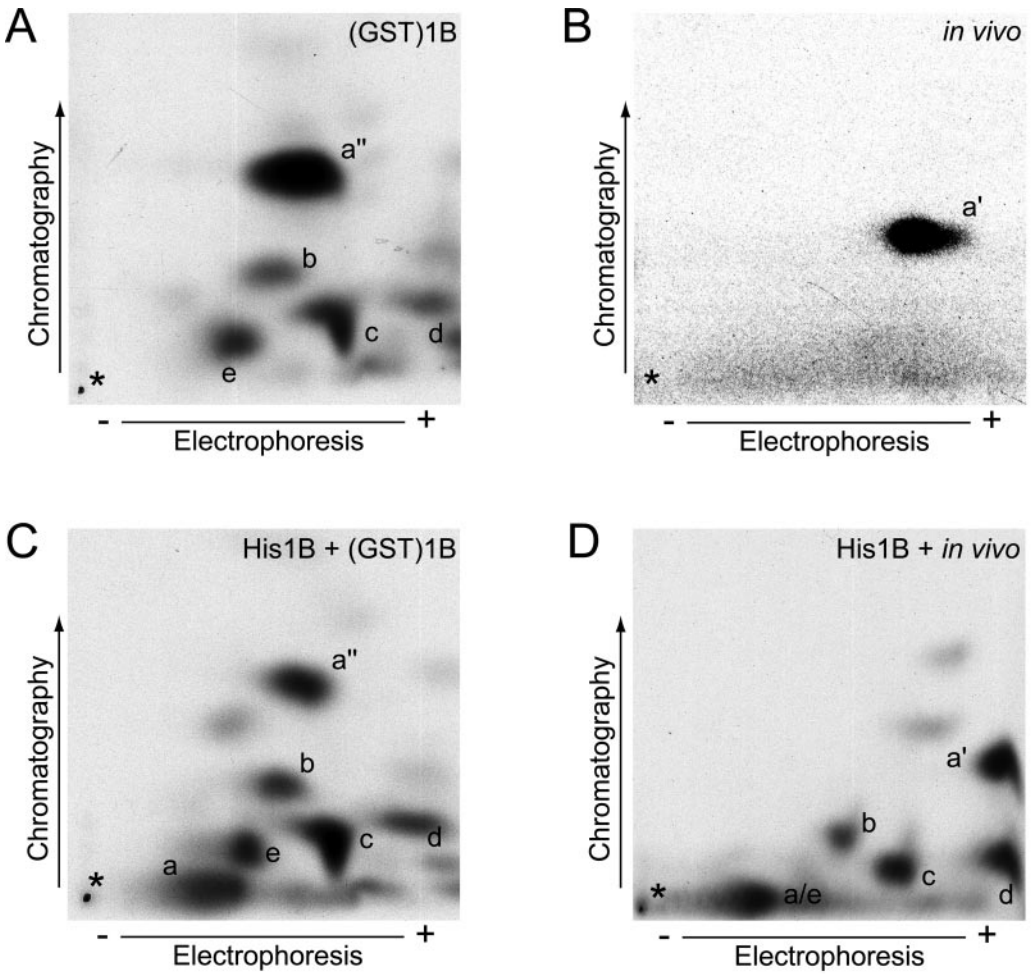

E

peptide	position (Dc, De)	sequence
His1B	a (0.020, 0.304)	GSHHHHHHGSM***S***
in vivo	a' (0.054, 0.325)	M***S***
(GST)1B	a" (0.031, 0.408)	GPLGSM***S***

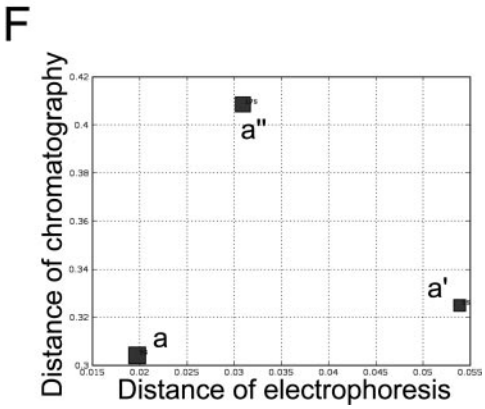

FIG. 4. **Coronin 1B is phosphorylated on an N-terminal site.** Tryptic peptide maps of (GST)1B (*A*), *in vivo* phosphorylated Coronin 1B (*B*), a mixture of His1B + (GST)1B (*C*), and a mixture of His1B + *in vivo* sample (*D*). *E*, sequences of N-terminal tryptic peptides of the various samples. Ser-2 is indicated with *bold* and *italics*. *F*, theoretical map of peptides from *E*.

correct molecular weight, whereas the S2A sample had no detectable band at the equivalent area of the gel. These samples were blotted with our Coronin 1B antibody to confirm that both proteins were present (data not shown). The tryptic peptide maps generated from the Coronin 1B-GFP bands exhibited a similar pattern of spots as the recombinant preparation studied previously (spots b–e). However, the wild-type sample did not exhibit peptides a or a″, but rather contained a peptide corresponding to a′. This spot was absent from the S2A sample (Fig. 5*C*). Together, these data indicate that Ser-2 is the major site phosphorylated by PKC on Coronin 1B *in vivo*.

Our experiments using PMA and PKC inhibitors demonstrated that phosphorylation of Coronin 1B regulates its interaction with the Arp2/3 complex. If Ser-2 is the critical phosphorylation site, then mutations in Ser-2 should modulate the Coronin 1B-Arp2/3 interaction. In addition to the S2A mutation described above, we also made a second mutant, S2D, in which Ser-2 was mutated to aspartic acid to mimic phosphorylated Coronin 1B. These mutants, along with the wild-type version, were transiently expressed in HEK293 cells and immunoprecipitated with GFP antibodies. The IP samples were blotted for p34-Arc to detect associated Arp2/3 complex. The

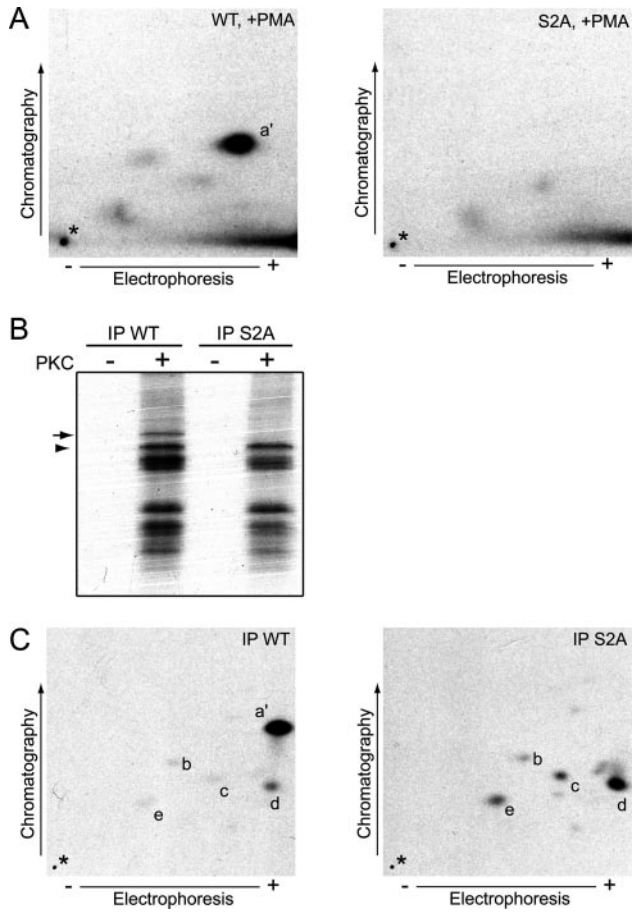

FIG. 5. **Ser-2 of Coronin 1B is the site directly phosphorylated by PKC *in vivo*.** *A*, *in vivo* phosphorylation of either wild-type (*WT*) or S2A mutant form of Coronin 1B expressed in HEK293 cells, and stimulated with 100 nM PMA. *B*, *in vitro* phosphorylation of immunoprecipitated wild-type or S2A mutant Coronin 1B tagged with GFP from unlabeled HEK293 cells by purified PKCα. *Arrow* indicates GFP-tagged Coronin and the *arrowhead* indicates PKCα autophosphorylation. *C*, tryptic peptide maps of GFP-tagged Coronins from *B*. Note the similar pattern of b, c, d, and e spots to *in vitro* samples from Fig. 4 and absence of the a′ spot in S2A mutant. Equal counts of both the wild-type and S2A samples were loaded on the TLC plates to reveal any detectable phosphorylation of peptide a′ in the S2A sample.

Coronin 1B S2A mutant showed a stronger interaction with the Arp2/3 complex relative to wild type, whereas the S2D mutant had weaker interaction (Fig. 6*A*). This trend is consistent with our observation that increasing Coronin 1B phosphorylation by PMA treatment decreases the interaction with Arp2/3. Interestingly, these mutants did not affect oligomerization of the GFP-tagged form with the endogenous Coronin 1B, suggesting that this interaction is not regulated by phosphorylation at Ser-2.

To further characterize these mutant versions of Coronin 1B, we created stable Rat2 cell lines expressing the mutants via retroviral transduction. These lines were sorted for equal levels of GFP expression by a fluorescence-activated cell sorter, and equal expression levels of Coronin 1B-GFP were verified by Western blotting (Fig. 6*B*). We looked for changes in Coronin 1B-Arp2/3 interactions in these cell lines by co-IP. Unlike the transiently transfected HEK293 cells, there was no increase in the p34-Arc interaction with the S2A mutant, but there was a reproducible decrease with the S2D mutant (Fig. 6*C*). When these IPs were probed with the $pSer^{PKC}$ antibody described above, we noted that the $pSer^{PKC}$ antibody does not cross-react with either the S2A or S2D mutant (Fig. 6*C*). These data demonstrate that this antibody specifically recognizes Coronin 1B phosphorylated on Ser-2. In cells expressing the S2A mutant, we observed a hyperphosphorylation of the endogenous Coronin 1B. This may reflect a compensatory mechanism in this stable cell line. Because phospho-Coronin 1B does not interact as well with Arp2/3, this may explain why we did not observe an increase in p34-Arc interaction in the S2A-expressing cell line. When we examined the localization of the mutants in these stable Rat2 lines, we saw no difference between either of the mutant proteins and the wild type Coronin 1B-GFP. There was also no discernable change in p34-Arc or F-actin staining with expression of the mutants (Fig. 6*B*). This suggests that phosphorylation of Coronin 1B does not affect its subcellular localization properties, although it is formally possible that the mutants are localizing via oligomerization with the endogenous Coronin 1B.

To address the importance of Ser-2 phosphorylation for Coronin 1B function, we used a PMA-induced ruffle formation assay. Previous studies indicated that PMA stimulation of serum-starved cells induces a transient activation of the Rac GTPase and that this Rac activity is required for PMA-induced ruffling activity (30, 31). In our stable Rat2 lines expressing wild-type or Ser-2-mutated Coronin 1B, we observed striking differences in the ability of PMA to induce ruffles in serum-starved cells (Table I). About 41% of the Rat2 control cells show ruffling at 10 min after stimulation, whereas 60% of cells overexpressing wild-type Coronin 1B show ruffling under the same conditions. Both the Rat2 control cells and wild-type Coronin 1B overexpressers had diminished ruffling by 30 min after stimulation, suggesting that this response adapts over time. Cells expressing the S2A mutant version of Coronin 1B had the highest level of ruffling (71%) at 10 min and had sustained high levels of ruffling at all time points tested. Interestingly, cells expressing the S2D mutant version of Coronin 1B had suppressed ruffling with only about 26% of cells showing ruffling activity at 10 min. The S2D cells did show a peak of ruffling activity at 20 min that returned to control levels by 30 min, suggesting that these cells have diminished ruffling rather than a total loss. Together, these data suggest that overexpression of wild-type or S2A Coronin 1B enhances the early phase of the ruffling response, and that Coronin 1B phosphorylation at Ser-2 may be a major factor in the adaptation of PMA-induced ruffling at later times. Furthermore, these data suggest that, consistent with its localization pattern, Coronin 1B exerts a strong effect on actin-dependent processes at the leading edge.

To further explore Coronin 1B function and the role of Ser-2 phosphorylation in regulating Coronin function, we turned to the single cell tracking assay. In this assay, individual cells undergoing random cell movement are tracked in time-lapse movies and information about speed and directional persistence are extracted. Overexpression of wild-type Coronin 1B caused a slight, but statistically significant increase in average cell speed (analysis of variance, $F = 106.7$, $p < 0.0001$; Dunnett's multiple comparison test, $p < 0.05$) (Fig. 7*A*). Expression of the S2A mutant caused a much stronger increase in cell speed, whereas expression of the S2D mutant suppressed cell speed below that of the parental Rat2 cells (Dunnett's multiple comparison test, $p < 0.01$). None of the cell lines showed significant differences in directional persistence (data not shown).

To understand the relative contribution of Ser-2 phosphorylation to the overall effect of PMA on cell migration, we first examined the dose relationship of PMA treatment to Coronin 1B phosphorylation by Western blotting. In this experiment, the cells were treated with PMA for 30 min in serum-containing media. For examining phosphorylation status, we used Rat2 cells expressing wild-type Coronin 1B tagged with GFP to

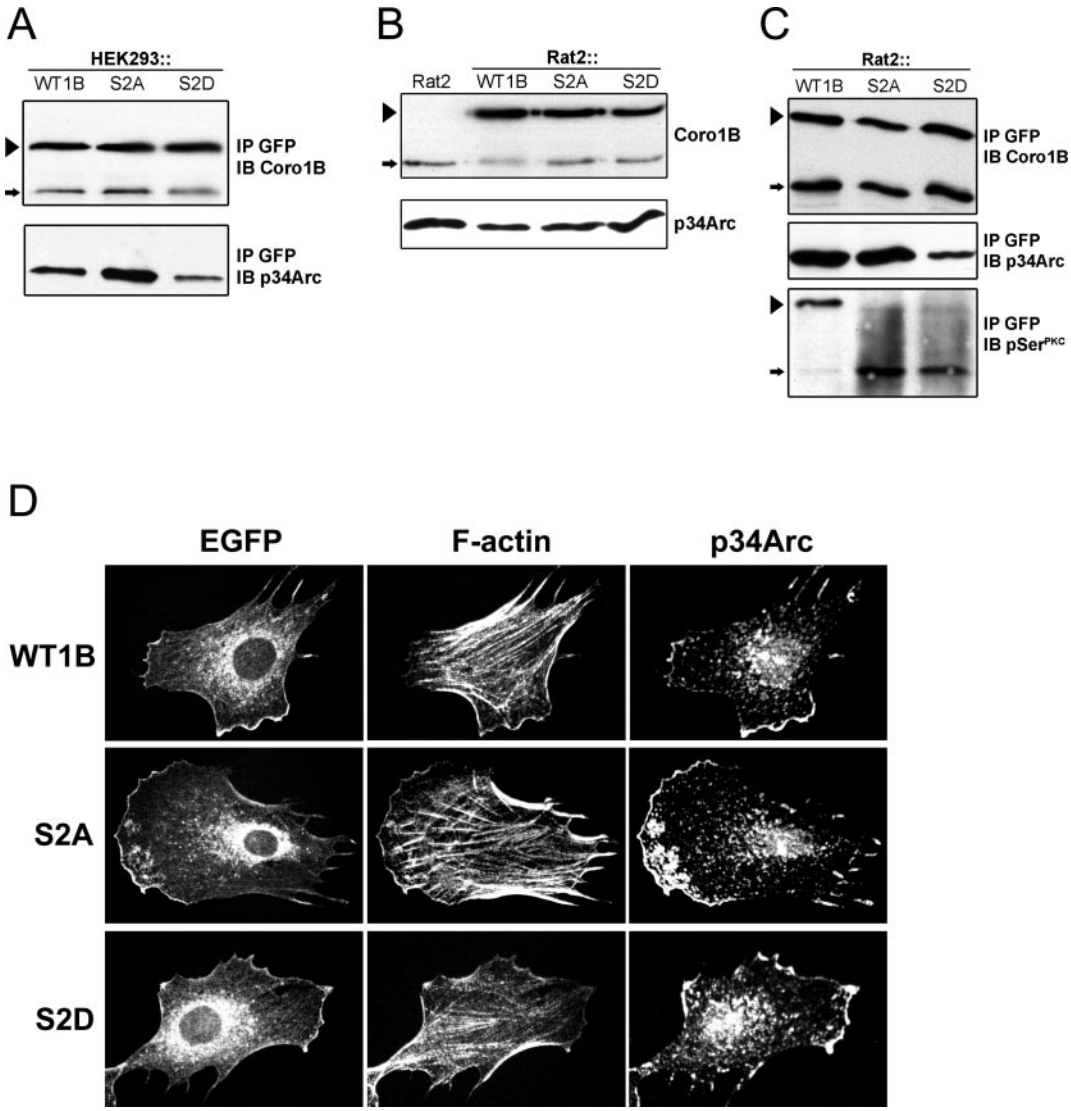

FIG. 6. **Ser-2 mutants affect the interaction between Coronin 1B and the Arp2/3 complex, but not subcellular localization.** *A*, transient transfection of Ser-2 mutants into HEK293 cells. Samples were immunoprecipitated with GFP antibody and blotted with Coro1B or p34-Arc antibodies. The *arrowhead* indicates GFP-tagged Coronin 1B, and the *arrow* indicates endogenous Coronin 1B. *B*, lysates from Rat2 stable cell lines expressing GFP-tagged wild-type, S2A, or S2D mutant Coronin 1B blotted as indicated. *C*, GFP IPs of samples in *B* blotted as indicated. Note the lack of cross-reactivity of $pSer^{PKC}$ antibody with either Ser-2 mutant. *D*, GFP-tagged Ser-2 mutants have the same localization pattern as the wild-type Coronin 1B in Rat2 cells. Cells were stained with antibodies to p34-Arc to label Arp2/3 and phalloidin to label F-actin.

TABLE I
PMA-induced ruffling response

Data presented are the combined results from two independent experiments. Cells were counted in 6 fields of view with ruffling cells/total, cells counted are reported in parentheses. Chi-square values for each time point range from 38.5 to 82.9, indicating that each time point contains statically significant deviation from expected Rat2 control proportion ($p < 0.000001$).

	Untreated	5 min	10 min	20 min	30 min
Rat2	13.4% (46/343)	38.4% (159/414)	41.4% (165/399)	52.2% (224/429)	38.8% (150/387)
WT1B	30.1% (64/213)	55.4% (185/334)	60.3% (188/312)	64.2% (280/436)	47.0% (236/502)
S2A	17.8% (40/225)	63.3% (209/330)	71.3% (268/376)	76.1% (331/435)	76.1% (299/393)
S2D	25.4% (63/248)	13.2% (38/287)	26.8% (110/410)	45.0% (172/382)	32.8% (168/513)

examine the phosphorylation of both the GFP-tagged and endogenous forms. Cells were stimulated with different doses of PMA and the Coronin 1B-GFP immunoprecipitated with GFP antibodies. These samples were blotted either with the $pSer^{PKC}$ antibody to detect phosphorylated Coronin 1B or the Coronin 1B antibody to detect total immunoprecipitated Coronin protein (Fig. 7*B*). Both GFP-tagged and endogenous Coronin 1B are phosphorylated in a dose-dependent manner with the greatest increase occurring between 1 and 5 nM PMA.

To address the importance of Ser-2 phosphorylation in mediating the effects on cell migration on PMA, we did a dose-response single cell tracking experiment in our cell lines expressing the wild-type or mutant forms of Coronin 1B (Fig. 7*C*). For Rat2 control cells, a steady decrease in cell speed was observed with increasing PMA dose. This is consistent with studies of other cells lines showing an inhibitory effect of PMA on cell speed (32). Cells overexpressing the wild-type Coronin 1B showed a similar overall dose-dependent decrease in cell speed, but showed a sharper drop between 1 and 5 nM PMA relative to controls. This is consistent with the phospho-specific

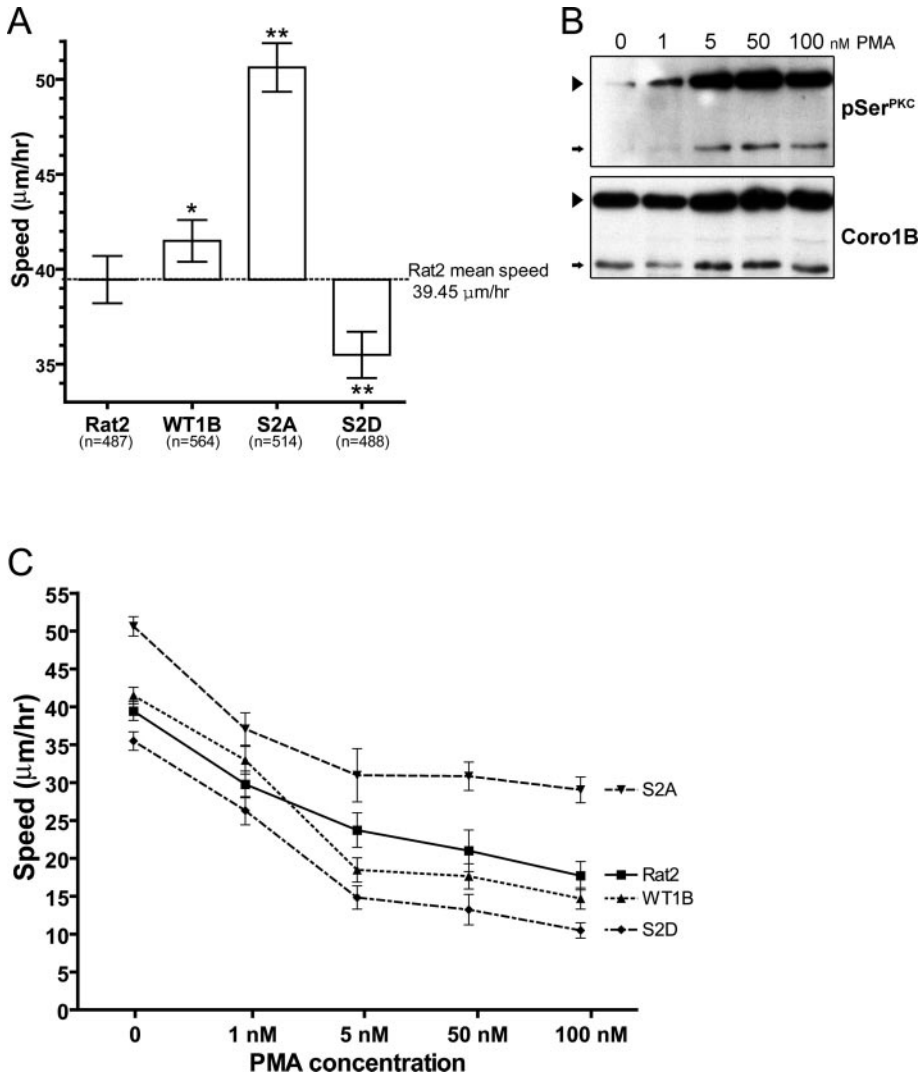

FIG. 7. **Phosphorylation of Coronin 1B at Ser-2 regulates cell migration.** *A*, migration speed of Rat2 stable cell lines measured by the single cell tracking method (number tracked per cell type in *parentheses*). Data were analyzed by one-way analysis of variance ($p < 0.0001$), and individual treatments were analyzed with Dunnett's multiple comparison post-test (*, $p < 0.05$; **, $p < 0.01$; *error bars* show 95% confidence intervals). *B*, PMA induces a dose-dependent increase in Coronin 1B phosphorylation. Rat2 cells expressing the GFP-tagged wild-type Coronin 1B were treated with the indicated dose of PMA for 30 min. Lysates were immunoprecipitated with GFP antibodies and blotted as indicated. The *arrowhead* indicates GFP-tagged Coronin 1B, and the *arrow* indicates endogenous Coronin 1B. *C*, migration speeds of Rat2 stable cell lines treated with different doses of PMA. Cells were treated with PMA for 30 min prior to the beginning of the movies and drug was present throughout. Speed was measured by the single cell tracking method (at least 100 cells tracked for each data point).

Western blot analysis where the sharpest increase in phosphorylation occurred between these two doses. Cells expressing the S2A mutant showed a dose-dependent decrease in cell speed to a point, but the decline in cell speed leveled off by 5 nM and showed no further decrease after this point. This suggests that a mutant version of Coronin 1B that cannot be phosphorylated confers partial resistance to the inhibitory effects of PMA on cell speed. Conversely, the S2D mutant rendered the cells hypersensitive to the inhibitory effects of PMA with the majority of the inhibitory effect occurring by the 5 nM dose. Together, these data indicate that Coronin 1B phosphorylation at Ser-2 plays a significant role in mediating the effects of PMA on cell migration speed in fibroblasts.

DISCUSSION

Coronins are a highly conserved family of proteins that regulate actin-dependent processes such as migration and endocytosis; however, little is known about the function or regulation of these molecules in mammalian systems. In this work, we show that Coronin 1B interacts *in vivo* with the Arp2/3 complex and that this interaction is inhibited by PKC phosphorylation. We have identified the single major *in vivo* phosphorylation site, Ser-2, and demonstrated that mutations in this site cause striking effects on fibroblast motility. In addition, we show that Coronin 1B phosphorylation mediates a significant fraction of PMA-induced changes in fibroblast motility.

Mammalian genomes contain at least six Coronin genes that can be broken down into three subclasses based on sequence homology, localization, and function.[2] Coronins 1A, 1B, and 1C form a distinct group and are most similar to the Coronin genes in single-cell eukaryotes. The *Coronin 1B* and *1C* genes are ubiquitously expressed, but *Coronin 1B* is expressed at 2–10-fold higher levels at the mRNA level depending on the tissue. This suggests that Coronin 1B may the predominant Coronin of this subclass in many cell types and tissues.

Because Coronin 1B is expressed at such high levels across tissues, we examined a number of molecular interactions that have been seen with other Coronins for this protein. First, our data show that Coronin 1B oligomerizes with itself and that this interaction is exclusively homo-oligomeric in nature. It will be interesting to see if all mammalian Coronins display this degree of specificity in their oligomerization. Second, like all other Coronins tested from any species, recombinant Coronin 1B co-sediments with F-actin *in vitro*.[2] Third, our reciprocal co-IP and co-localization data show that Coronin 1B interacts *in vivo* with the Arp2/3 complex in all cell types tested. Furthermore, we see similar interactions between Coronin 1C and Arp2/3.[3] Whereas Coronin 1A was identified as a major co-purifying protein in preparations of the Arp2/3 complex from neutrophils, the data reported in this work are the first to directly confirm that the Coronin-Arp2/3 interaction, first dem-

[3] N. Holoweckyj and J. E. Bear, unpublished observation.

onstrated in yeast, is conserved in mammals.

Our data are the first direct demonstration that phosphorylation regulates Coronin function. Other groups have reported PKC phosphorylation of Coronins 1A and 1B and, for Coronin 1A, there is an increased localization of the protein on phagosomes in HL-60 cells treated with high doses of PKC inhibitors, but none of these studies directly shows regulation by phosphorylation (12, 13). Our studies reveal that the *in vivo* interaction between Coronin 1B and Arp2/3 is strongly inhibited by PKC phosphorylation. We mapped the major *in vivo* PKC phosphorylation site on Coronin 1B to Ser-2 using tryptic peptide analysis and confirmed this result using site-directed mutagenesis. Expressing Ser-2 mutants has striking effects on fibroblast motility. The S2A mutant has stronger interaction with Arp2/3, and increases PMA-induced ruffling and cell speed relative to the wild-type Coronin 1B, suggesting that this mutant is constitutively active. Conversely, the S2D mutant has reduced interaction with Arp2/3, inhibits ruffling, and suppresses cell speed below that of the parental Rat2 cells, suggesting that this mutation creates a dominant negative Coronin.

Although our data shows regulation of Coronin function by PKC, several outstanding issues remain to be resolved. The precise isoform or isoforms of PKC that phosphorylate Coronin 1B *in vivo* remain to be delineated. Furthermore, the upstream signaling pathways that ultimately regulate Coronin 1B phosphorylation also remain unclear. In rabbit parietal cells, carbachol (a muscarinic agonist) stimulates Coronin 1B phosphorylation (13), but we were unable to stimulate Coronin 1B phosphorylation in HEK293 cells with this agonist (data not shown). However, this may simply reflect poor/absent expression of the necessary receptor or G-protein in this cell type. A second unresolved issue concerning the PKC regulation of Coronin 1B function is the nature of the dominant negative effect observed with the S2D mutant. At least two possible explanations could account for this effect. First, this pseudo-phosphorylated version may be non-functional, but still able to bind to and sequester key Coronin 1B binding partners. Second, phospho-Coronin 1B may have a distinct function from the dephospho-form that does not involve Arp2/3 and is inhibitory for ruffling and migration. More experiments will be needed to resolve these issues.

Whereas the mechanistic details of mammalian Coronin function remain unclear, it is worth considering data on Coronin function from yeast in developing a working hypothesis about Coronin 1B function in mammalian cell motility. In yeast, Coronin binds directly to the Arp2/3 complex *in vitro* and, more specifically, to the p35-Arc subunit in two-hybrid assays (6). When added to *in vitro* polymerization assays, Coronin inhibits the Arp2/3-mediated nucleation of actin filaments. Recent structural data indicate that the addition of Coronin to Arp2/3 preparations (visualized by EM and single particle reconstruction) causes Arp2/3 to adopt an open or inactive conformation (33). Together, these data led the Goode laboratory (33) to propose that yeast Coronin is a direct inhibitor of the Arp2/3 complex. Our data indicate that overexpression of the mutant form of Coronin 1B (S2A) that interacts more robustly with Arp2/3 drives the actin-dependent processes of membrane ruffling and cell migration.

Superficially, these datasets seem inconsistent, but there are a number of possible models in which both could be correct or at least consistent within a particular cellular context. One possibility is that Coronin inhibits Arp2/3 activity in both yeast and mammalian cells, but that in fibroblasts, this results (indirectly) in the disassembly of actin networks through other mechanisms such as ADF/cofilin. This would result in accelerated actin network turnover, and that could lead to enhanced cell motility. Such a mechanism would be consistent with the genetic synergy between mutations in the Coronin and Cofilin genes in yeast (5). Another possibility is that Coronin recruits inactive Arp2/3 to the sides of actin filaments at specific locations within cells where it can be acted upon by activators such SCAR/WASP proteins as previously suggested (6). Phosphorylation of Coronin (and subsequent loss of interaction with Arp2/3) could act as a switch to expose "activable" Arp2/3 that had been previously docked on filaments at specific locations within the cell. Neither of these models, however, completely explains why Coronin is a biochemical inhibitor of Arp2/3, but a cellular "activator" of Arp2/3-dependent processes such as membrane ruffling and cell migration in fibroblasts. Alternately, mammalian Coronins and yeast Coronin may both interact with Arp2/3, but have evolved divergent mechanisms for regulating the complex. Experiments are underway to rigorously test these and other possible models.

One of our most striking findings is that Coronin 1B phosphorylation mediates a significant fraction of effects of PMA on fibroblast ruffling and migration. This is a somewhat surprising result because PMA activates all of the conventional and novel isoforms of PKC, and likely stimulates the phosphorylation of a large number of protein substrates. When considering our results with PMA, it is important to take into account the precise conditions of treatment and the different phenomenon being observed. The PMA-induced ruffling is highly dependent on serum starvation and may represent a different effect than the 2–3-h treatments in the presence of serum that we used for the cell tracking studies. Our ruffling data are consistent with Coronin 1B playing at least two distinct roles in this process. First, overexpression of wild-type (or S2A) Coronin 1B enhances the PMA-induced ruffling response that is initiated by an unknown PMA target and presumably involves a Rac-dependent pathway. Second, subsequent phosphorylation of Coronin 1B appears to be critical for an adaptation of the PMA-induced ruffling response as demonstrated by the sustained ruffling observed in the cells expressing the S2A mutant. In the cell tracking experiments, PMA was added 30 min before the start of the movies in the presence of serum. This treatment did not induce continuous ruffling, but rather seemed to cause a dose-dependent reduction of the polarized morphology normally seen in migrating fibroblasts. The reduction in cell speed likely arises from the failure to maintain the polarized morphology necessary for effective migration. Expression of the S2A mutant version of Coronin 1B partially protected the cells from this loss of polarity induced by PMA (data not shown). This suggests that, in this assay, Coronin 1B phosphorylation may have an important role in regulating cell polarity. Future experiments will explicitly test this hypothesis.

Acknowledgments—We thank Frank Gertler for support in this project. We also thank Ned Sharpless and Janakiraman Krishnamurthy for the mouse RNAs and help setting up quantitative real-time PCR, Matt Welch for p41 antibodies, Brian Harms for sharing Matlab macros for calculating directional persistence, and Bruce Goode, Kris DeMali, Tom Marshall, and Carol Otey for helpful discussions and comments on the manuscript.

REFERENCES

1. de Hostos, E. L., Bradtke, B., Lottspeich, F., Guggenheim, R., and Gerisch, G. (1991) *EMBO J.* **10,** 4097–4104
2. de Hostos, E. L., Rehfuess, C., Bradtke, B., Waddell, D. R., Albrecht, R., Murphy, J., and Gerisch, G. (1993) *J. Cell Biol.* **120,** 163–173
3. Hacker, U., Albrecht, R., and Maniak, M. (1997) *J. Cell Sci.* 110, 105–112
4. Heil-Chapdelaine, R. A., Tran, N. K., and Cooper, J. A. (1998) *Curr. Biol.* **8,** 1281–1284
5. Goode, B. L., Wong, J. J., Butty, A. C., Peter, M., McCormack, A. L., Yates, J. R., Drubin, D. G., and Barnes, G. (1999) *J. Cell Biol.* **144,** 83–98
6. Humphries, C. L., Balcer, H. I., D'Agostino, J. L., Winsor, B., Drubin, D. G., Barnes, G., Andrews, B. J., and Goode, B. L. (2002) *J. Cell Biol.* **159,** 993–1004
7. Bharathi, V., Pallavi, S. K., Bajpai, R., Emerald, B. S., and Shashidhara, L. S.

(2004) *J. Cell Sci.* 117, 1911–1922
8. Mishima, M., and Nishida, E. (1999) *J. Cell Sci.* **112,** 2833–2842
9. Asano, S., Mishima, M., and Nishida, E. (2001) *Genes Cells* **6,** 225–235
10. de Hostos, E. L. (1999) *Trends Cell Biol.* **9,** 345–350
11. Nal, B., Carroll, P., Mohr, E., Verthuy, C., Da Silva, M. I., Gayet, O., Guo, X. J., He, H. T., Alcover, A., and Ferrier, P. (2004) *Int. Immunol.* **16,** 231–240
12. Itoh, S., Suzuki, K., Nishihata, J., Iwasa, M., Oku, T., Nakajin, S., Nauseef, W. M., and Toyoshima, S. (2002) *Biol. Pharm. Bull.* **25,** 837–844
13. Parente, J. A., Jr., Chen, X., Zhou, C., Petropoulos, A. C., and Chew, C. S. (1999) *J. Biol. Chem.* **274,** 3017–3025
14. Di Giovanni, S., De Biase, A., Yakovlev, A., Finn, T., Beers, J., Hoffman, E. P., and Faden, A. I. (2005) *J. Biol. Chem.* **280,** 2084–2091
15. Spoerl, Z., Stumpf, M., Noegel, A. A., and Hasse, A. (2002) *J. Biol. Chem.* **277,** 48858–48867
16. Fridman, R., Lacal, J. C., Reich, R., Bonfil, D. R., and Ahn, C. H. (1990) *J. Cell. Physiol.* **142,** 55–60
17. Jackson, D., Zheng, Y., Lyo, D., Shen, Y., Nakayama, K., Nakayama, K. I., Humphries, M. J., Reyland, M. E., and Foster, D. A. (2005) *Oncogene* **24,** 3067–3072
18. Ng, T., Shima, D., Squire, A., Bastiaens, P. I., Gschmeissner, S., Humphries, M. J., and Parker, P. J. (1999) *EMBO J.* **18,** 3909–3923
19. Dugina, V. B., Svitkina, T. M., Vasiliev, J. M., and Gelfand, I. M. (1987) *Proc. Natl. Acad. Sci. U. S. A.* **84,** 4122–4125
20. Glowacka, D., Ginty, D. D., and Wagner, J. A. (1992) *J. Neurosci. Res.* **31,** 263–272
21. Taunton, J., Rowning, B. A., Coughlin, M. L., Wu, M., Moon, R. T., Mitchison, T. J., and Larabell, C. A. (2000) *J. Cell Biol.* **148,** 519–530
22. Overbergh, L., Giulietti, A., Valckx, D., Decallonne, R., Bouillon, R., and Mathieu, C. (2003) *J. Biomol. Tech.* **14,** 33–43
23. Bear, J. E., Loureiro, J. J., Libova, I., Fassler, R., Wehland, J., and Gertler, F. B. (2000) *Cell* **101,** 717–728
24. Ziegler, W. H., Tigges, U., Zieseniss, A., and Jockusch, B. M. (2002) *J. Biol. Chem.* **277,** 7396–7404
25. Boyle, W. J., van der Geer, P., and Hunter, T. (1991) *Methods Enzymol.* **201,** 110–149
26. Luo, K. X., Hurley, T. R., and Sefton, B. M. (1991) *Methods Enzymol.* **201,** 149–152
27. Oku, T., Itoh, S., Ishii, R., Suzuki, K., Nauseef, W. M., Toyoshima, S., and Tsuji, T. (2005) *Biochem. J.* **387,** 325–331
28. Wilkinson, S. E., Parker, P. J., and Nixon, J. S. (1993) *Biochem. J.* **294,** 335–337
29. Martiny-Baron, G., Kazanietz, M. G., Mischak, H., Blumberg, P. M., Kochs, G., Hug, H., Marme, D., and Schachtele, C. (1993) *J. Biol. Chem.* **268,** 9194–9197
30. Kurokawa, K., Itoh, R. E., Yoshizaki, H., Nakamura, Y. O., and Matsuda, M. (2004) *Mol. Biol. Cell* **15,** 1003–1010
31. Ridley, A. J., Paterson, H. F., Johnston, C. L., Diekmann, D., and Hall, A. (1992) *Cell* **70,** 401–410
32. Keller, H. U., Zimmermann, A., and Niggli, V. (1989) *Int. J. Cancer* **44,** 934–939
33. Rodal, A. A., Sokolova, O., Robins, D. B., Daugherty, K. M., Hippenmeyer, S., Riezman, H., Grigorieff, N., and Goode, B. L. (2005) *Nat. Struct. Mol. Biol.* **12,** 26–31